

Electronic Supporting Information (ESI)

Stoichiometry dependent mechanical properties of pyrogallol-isonicotinamide cocrystals

*Priyasha Harsha^a and Dinabandhu Das^{*a}*

School of Physical Sciences, Jawaharlal Nehru University, New Delhi-110067, India

Email: jnu.dinu@gmail.com

Table of Content

- 1) Experimental Section**
 - a) FT-IR Spectra**
- 2) Powder X-Ray Diffraction**
- 3) Thermo-gravimetric analysis (TGA)**
- 4) Differential Scanning Calorimetry (DSC)**
- 5) Crystallographic Parameters**
- 6) Hydrogen bonding parameters**
- 7) Energy calculations figures and tables**
- 8) Crystal Morphology with Face indices**
- 9) Thermal ellipsoid plot of the asymmetric unit**
- 10) Calculation of Elastic Strain**
- 11) Description of Videos (Video S1, S2 and S3)**
- 12) References**

1) Experimental Section

- **Synthesis of PGINMI12 and PGINMI21 cocrystal.**

PGINMI12 and **PGINMI21**, were prepared using the reported method.¹ In 1:2 cocrystal, 12.5 mg (0.1 mmol) **PG** and 24 mg (0.2 mmol) **INMI** and in 2:1 cocrystal 25 mg (0.2 mmol) **PG** and 12 mg (0.1 mmol) **INMI** were mixed in 8 mL of the same warm 1:1 ethyl acetate-toluene mixture. The mixture was allowed to set for few days for crystallisation. Needle and block shaped colourless crystals were obtained after crystallisation. The synthesized compounds were characterized by FT- IR and Powder X-ray Diffraction.

a) FT-IR Spectra

Transmission infrared spectra of the solids were obtained using a Fourier–transform infrared spectrometer (Shimadzu), 43 scans were collected at 4 cm⁻¹ resolution for each sample. The spectra were measured over the range of 4000-400 cm⁻¹.

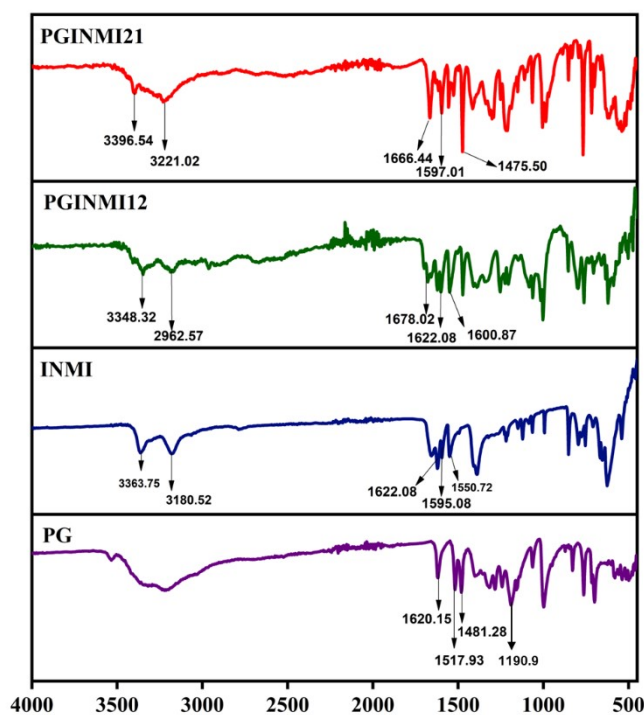
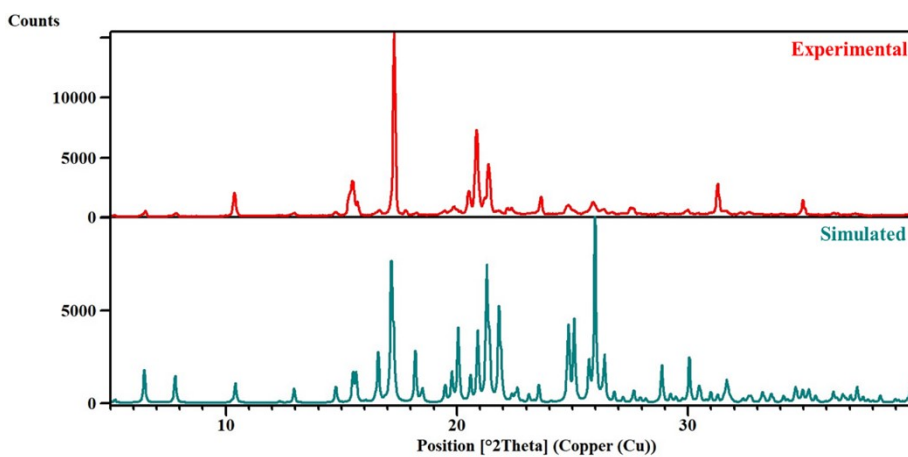


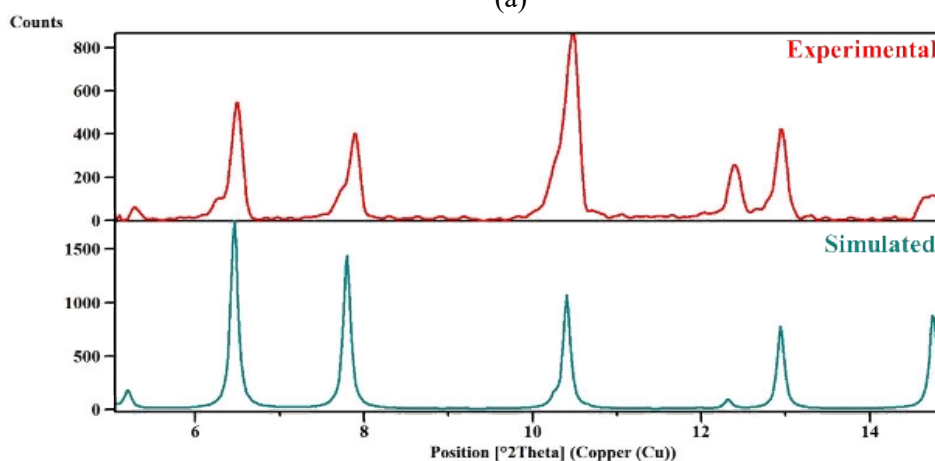
Figure S1 IR spectrum of **PGINMI21**, **PGINMI12**, **INMI** and **PG**.

2) Powder Xray Diffraction Pattern

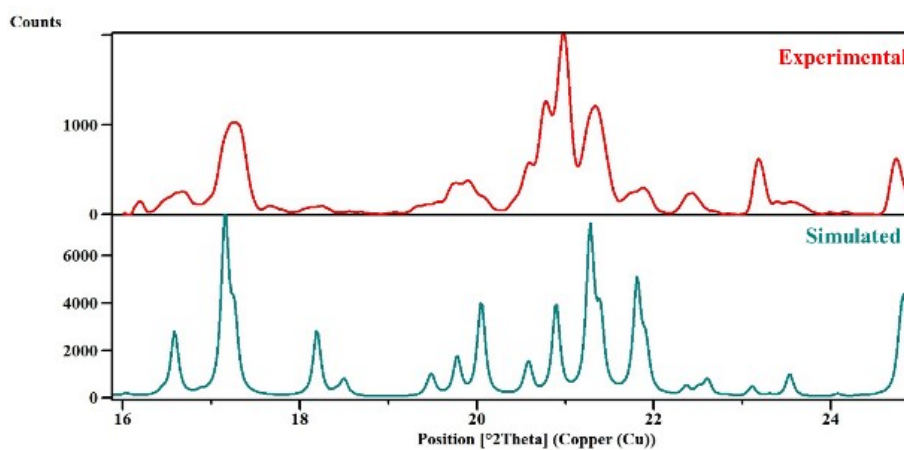
Powder X-ray diffractogram was measured on Rigaku powder X-ray diffractometer (Miniflex600 with Cu K α radiation, $\lambda = 1.54059 \text{ \AA}$) operating in Bragg–Brentano geometry. Crystals of the compound was crushed gently and layered on a sample holder. Data was recorded at room temperature at a scan rate of $2^\circ/\text{min}$ from 5° to 40° (2θ value).



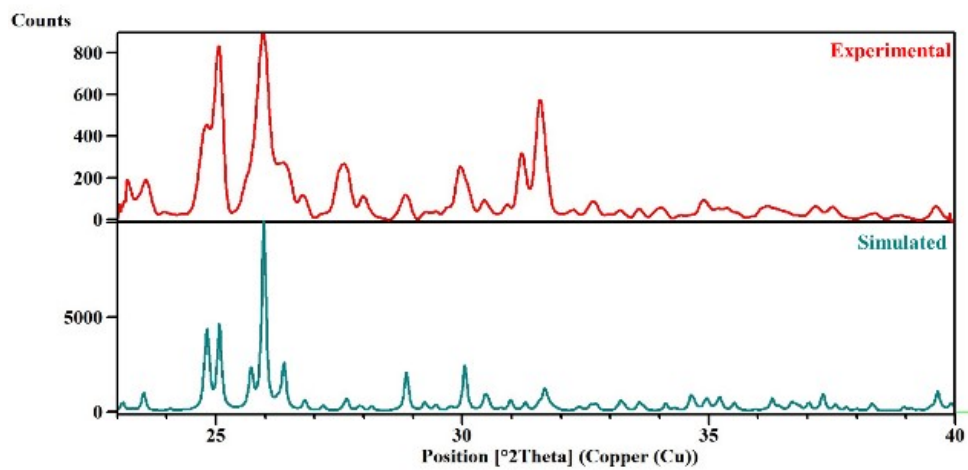
(a)



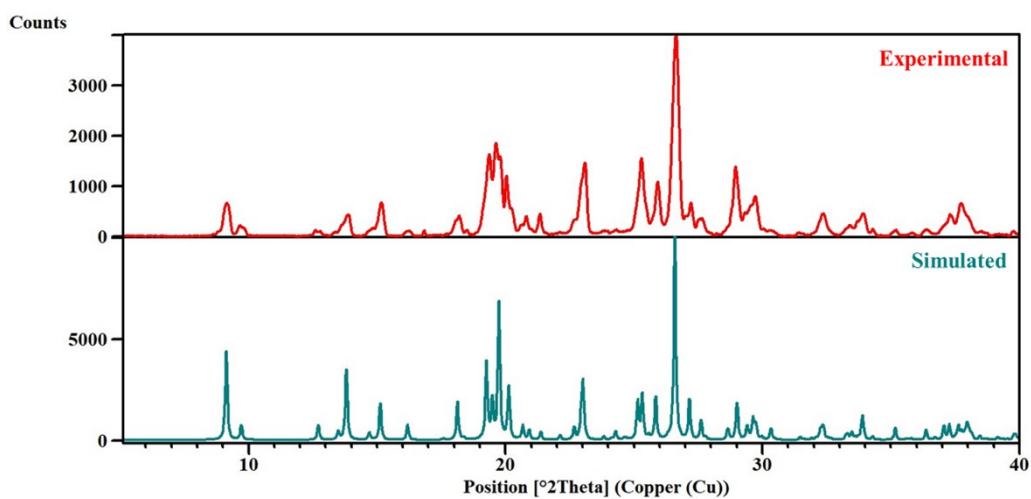
(b)



(c)



(d)



(e)

Figure S2 Powder X-ray Diffraction pattern of bulk samples of cocrystals (red) and simulated pattern obtained from SCXRD data (teal); (a) **PGINM12** (5° - 40°); (b) **PGINM12** (16° - 25°); (c) **PGINM12** (23° - 40°); (e) **PGINMI21** (red) and simulated pattern obtained from SCXRD data (teal).

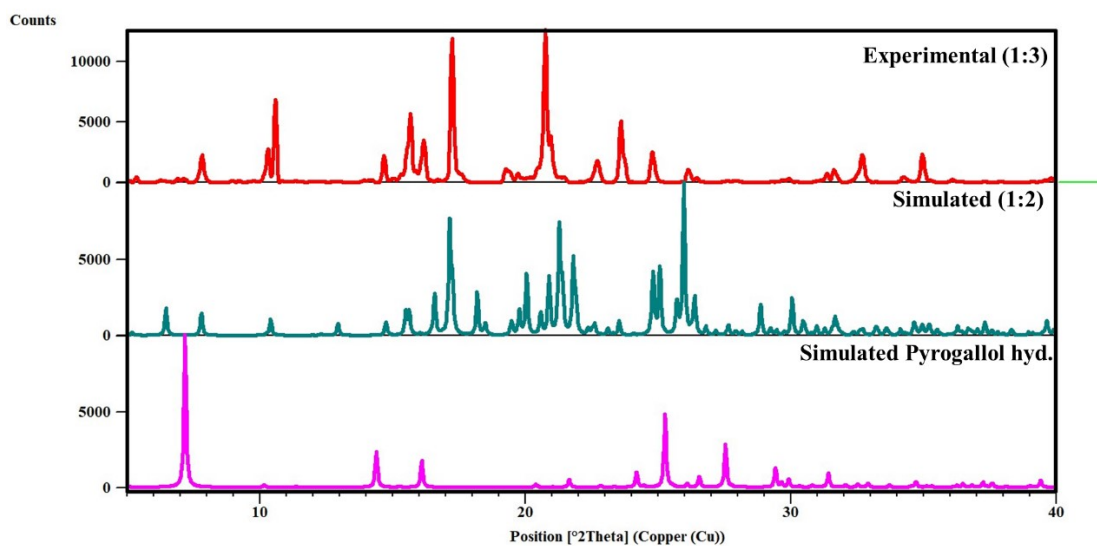


Figure S3 Powder X-ray Diffraction pattern of bulk samples of 1:3 ratio of **PG and INMI** cocrystals (red), simulated pattern obtained from SCXRD data (teal) of **PGINMI12** and **PG Hydrate**.

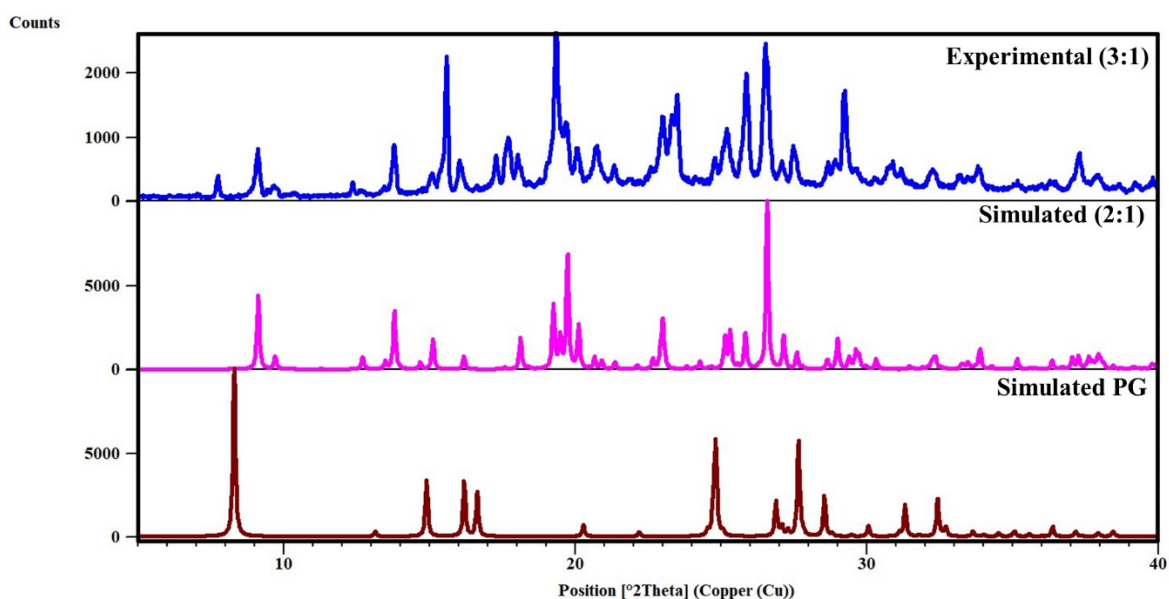


Figure S4 Powder X-ray Diffraction pattern of bulk samples of 3:1 ratio of **PG and INMI** cocrystals (blue), simulated pattern obtained from SCXRD data (Pink) of **PGINMI21** and **PG**.

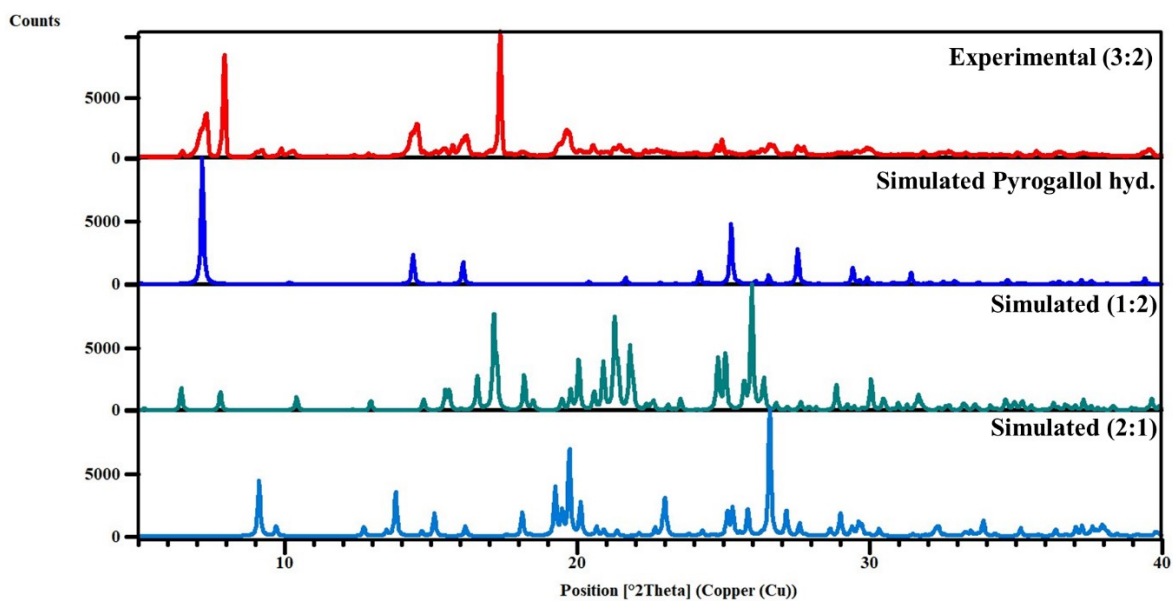


Figure S5 Powder X-ray Diffraction pattern of bulk samples of 3:2 ratio of PG and INMI cocystals (red), simulated pattern obtained from SCXRD of PG Hydrate (dark blue), PGINMI12 (teal) and PGINMI21 (light Blue).

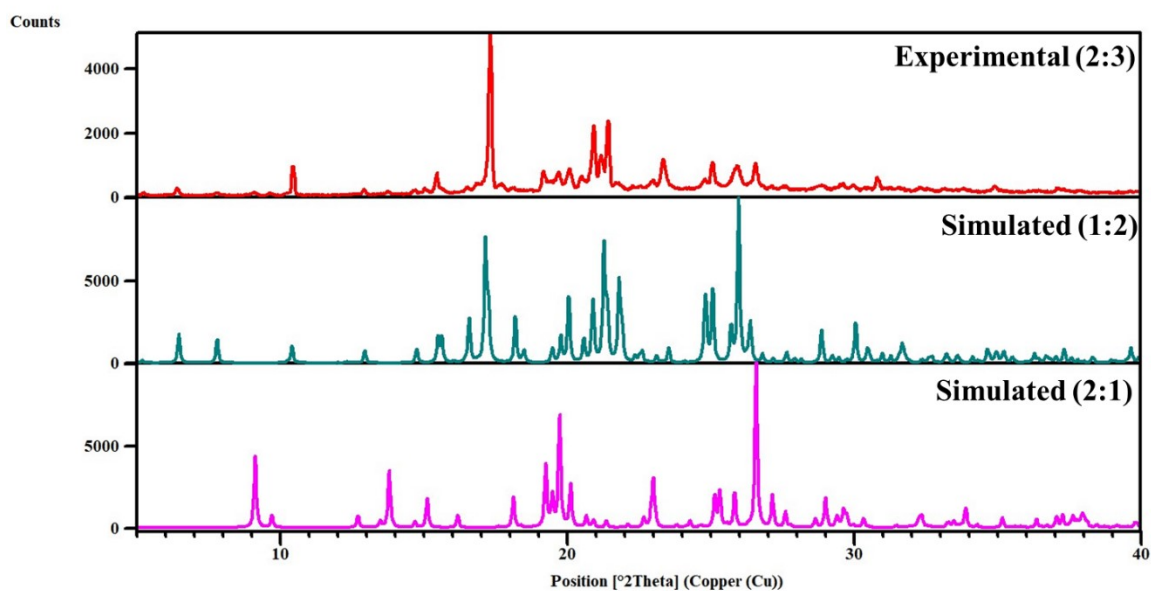
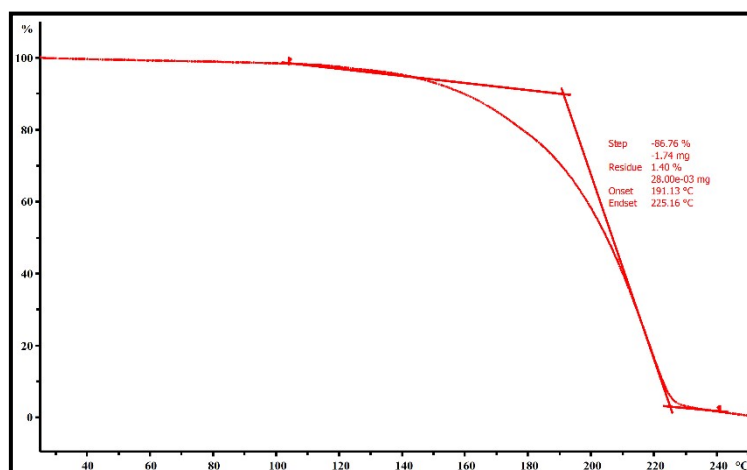


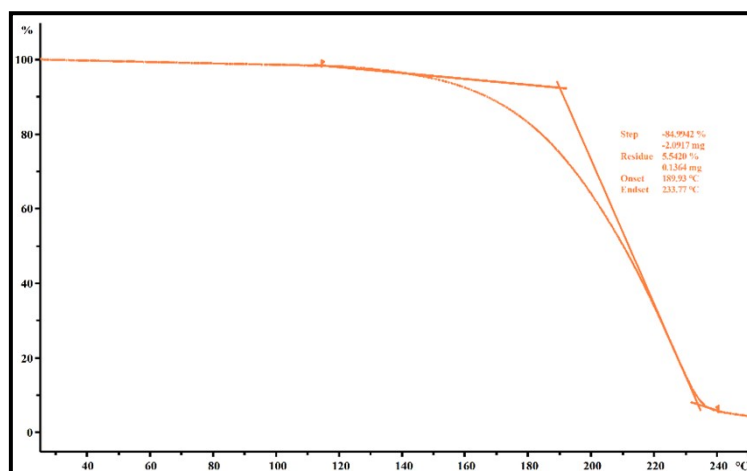
Figure S6 Powder X-ray Diffraction pattern of bulk samples of 2:3 ratio of PG and INMI cocystals (red) and simulated pattern obtained from SCXRD data of PGINMI12 (teal) and PGINMI21 (Pink).

3) Thermo-gravimetric analysis (TGA)

The TGA measurement of **PGINMI12** and **PGINMI21** was performed on Mettler Toledo equipped with Minichiller MT/230 from 25° to 250°C under nitrogen atmosphere (flow rate:20 ml /minute and at a scan rate of 5 °C / min.), using a software STARe version 13.00.



(a)



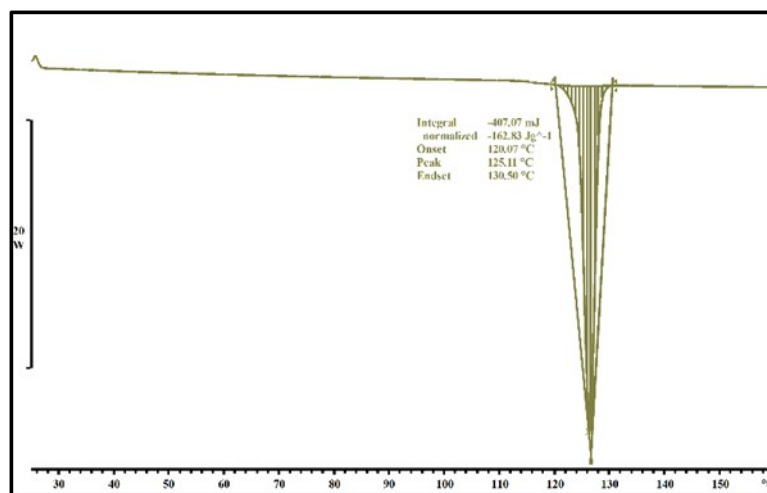
(b)

Figure S7 (a) TGA graph of **PGINMI12** showing thermal stability up to 191.13°C (b) **PGINMI21** showing thermal stability up to 189.93°C.

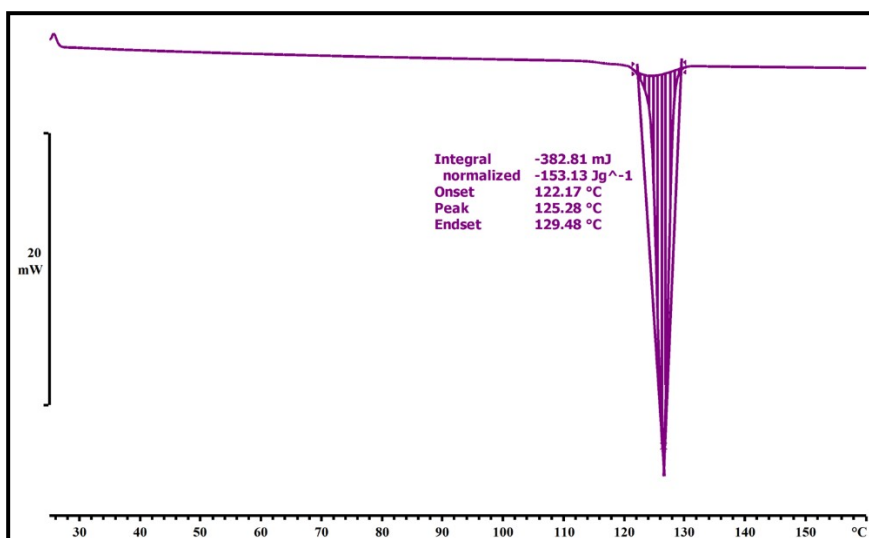
4) Differential scanning calorimetry (DSC)

The differential scanning calorimetric (DSC) measurement has been carried out in a sealed aluminium pan in the Mettler-Toledo DSC instrument. The instrument was equipped with HUBER TC100-MT chiller and STARe software version 13.00. The measurement was carried

out from 25°C to 180°C at the heating rate of 5°C/min under a N₂ gas segment with a flow rate of 20ml/min.



(a)



(b)

Figure S8 DSC thermogram of (a) PGINMI12 and (b) PGINMI21.

5) Single crystal X-Ray Diffraction

Although all the crystal structure of the cocrystals were already reported in the literature.¹ To study the mechanical properties crystal structure of these cocrystals were redetermined in Bruker D8 Quest single crystal X-ray diffractometer equipped with a microfocus anode (MoK α) and a PHOTON 100 CMOS detector. The integration and scaling of data were performed using

the SAINT programs.² Both structures were solved by direct methods and refined by full-matrix least-squares on F² using SHELX-2014.³ All non-hydrogen atoms were refined anisotropically. All the aromatic hydrogen atoms were placed using calculated positions on riding models.

Table S1 Crystallographic data of crystals and structure refinement parameters of **PGINMI12** and **PGINMI21**.

Identification code	PGINMI12	PGINMI21
Moiety formula	C ₃₆ H ₃₆ N ₈ O ₁₀	C ₁₈ H ₁₈ N ₂ O ₇
Crystal formula	Monoclinic	Triclinic
Space group	<i>P</i> 2 ₁	<i>P</i> -1
<i>a</i> (Å)	17.296(3)	9.2816(11)
<i>b</i> (Å)	5.8050(9)	9.6431(10)
<i>c</i> (Å)	18.263(3)	10.1781(10)
α (°)	90	72.635(3)
β (°)	100.708(5)	83.185(4)
γ (°)	90	80.135(4)
V/Å ³	1801.7(5)	854.39(16)
Z	4	2
<i>D</i> _{cal} /g cm ⁻³	1.365	1.455
T/K	300(2)	300(2)
μ /mm ⁻¹	0.102	0.114
<i>F</i> ₀₀₀	776	392
Reflection measured	39135	19712
Unique reflections	8959	5237
Observed reflections	8258	4221
Parameters	631	276
R _{int}	0.0420	0.0452
Final R (I>2 σ (I))	0.0356	0.0390
Final R(all data)	0.0393	0.0570

GOF on F ²	1.039	1.037
-----------------------	-------	-------

6) Hydrogen bonding parameters

Table S2 Hydrogen bonding parameter in the **PGINMI12** and **PGINMI21**.

Name of compounds	D(I)–H(I)···A(I) (Å)	D–H (Å)	H···A (Å)	D–A (Å)	∠ D–H···A (°)
PGINMI12	N(5)–H(6)···O(7)	0.91(3)	2.18(3)	3.060(3)	164(3)
	N(7)–H(27)···O(7)	0.88(3)	2.04(3)	2.884(2)	161(3)
	O(5)–H(37)···O(7)	0.87(3)	2.00(3)	2.810(2)	154(3)
	O(4)–H(25)···N(3)	0.90(3)	1.86(3)	2.750(2)	169(3)
	O(6)–H(30)···N(4)	0.90(3)	1.84(3)	2.725(3)	167(3)
	O(2)–H(23)···O(9)	0.92(3)	1.91(3)	2.757(2)	152(3)
	O(1)–H(29)···N(1)	0.88(4)	1.872(4)	2.727(3)	161(3)
	O(1)–H(31)···N(8)	0.90(4)	2.182(3)	2.964(3)	144(3)
	N(6)–H(17)···O(10)	0.84(3)	2.09(3)	2.895(3)	161(4)
	N(7)–H(2)···O(8)	0.87(3)	2.10(3)	2.914(3)	157(2)
	C(21)–H(16)···O(4)	0.95(2)	3.02(3)	3.331(2)	101(2)
	C(34)–H(21)···O(6)	0.98(3)	2.77(3)	3.143(2)	103(2)
	C(17)–H(12)···O(3)	0.97(3)	3.00(3)	3.304(3)	100(2)
C(22)–H(1)···O(8)	0.99(3)	2.62(3)	3.662(3)	160(2)	
PGINMI21	O(6)–H(6A)···N(1)	0.95(2)	1.72(2)	2.666(1)	176(2)
	N(2)–H(2)···O(5)	0.94(2)	1.98(2)	2.919(1)	173(2)
	O(4)–H(4A)···O(3)	0.87(2)	1.89(2)	2.750(2)	168(2)
	O(1)–H(1A)···O(7)	0.87(2)	1.98(2)	2.845(1)	178(2)
	O(2)–H(2A)···O(6)	0.86(2)	2.19(2)	2.900(2)	140(2)
	O(3)–H(3A)···O(7)	0.85(3)	1.93(3)	2.759(2)	162(2)
	C(17)–H(17)···O(4)	0.93(3)	2.87	3.713(2)	151.36
	C(14)–H(14)···O(5)	0.93	2.43	3.281(2)	151.75

Note: All values are calculated from PLATON⁴

Table S3 C–H···π parameters of **PGINMI12** and **PGINMI21**

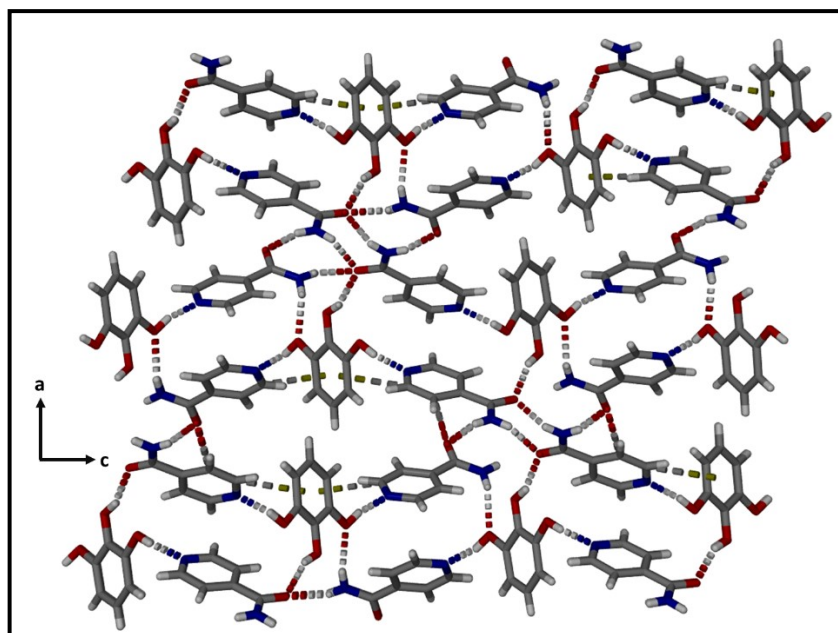
Name of compounds	D(I)–H(I)⋯A(I) (Å)	D–H (Å)	H⋯A (Å)	D–A (Å)	∠ D–H⋯A (°)
PGINMI12	C(14)–H(7) ⋯Cg1	0.94(3)	2.844	3.735	158.27
	C(29)–H(18) ⋯Cg1	0.90(3)	2.574	3.414	155.20
	C(19)–H(9) ⋯Cg2	0.98(3)	2.448	3.411	168.38
	C(31)–H(5) ⋯Cg2	0.92(3)	2.715	3.593	159.10
PGINMI21	C(5)–H(5) ⋯Cg1	0.930	2.959	3.706	138.29
	C(5)–H(5) ⋯ π*	0.930	3.062	3.805	138.00
	C(10)–H(10) ⋯ π**	0.930	3.133	3.850	135.28

Note * centroid of C(11) and C(12) is considered as π

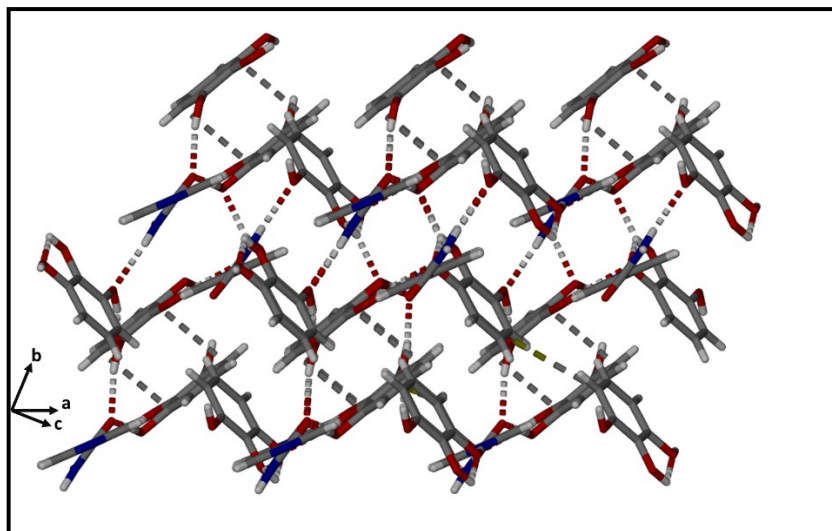
** centroid of C(5) and C(6) is considered as π

Table S4 π ⋯ π distance in PGINMI21

Cg(1)–Cg(1)	π ⋯ π parameters (Å)
C(3)–C(6)	3.446



(a)



(b)

Figure S9 (a) Crystal structure packing of **PGINMI12** with all interactions. (b) Crystal structure packing of **PGINMI21** with all interactions.

7) Energy calculations figures and tables

The energy calculations of all the crystal structures are done by using Crystal Explorer 21.5.⁵ Pairwise interaction energies in high Z' structures were calculated by growing cluster of 3.8Å radii of each independent molecule present in the asymmetric unit. In all the structures, the energy-display tube size (scale factor) was 80 and the energy cutoff was selected at 3 kJ mol⁻¹ for better visualization. Interaction energy calculations of the single crystals of **PGINMI21** and **PGINMI12** were carried out using unperturbed method CE-B3LYP/6-31g (d, p) energy model. In **PGINMI12**, six unique molecules are present in the unit cell and each molecule has been grown within in radius of 3.8Å for calculating total interaction energies (Figure S7-S13).

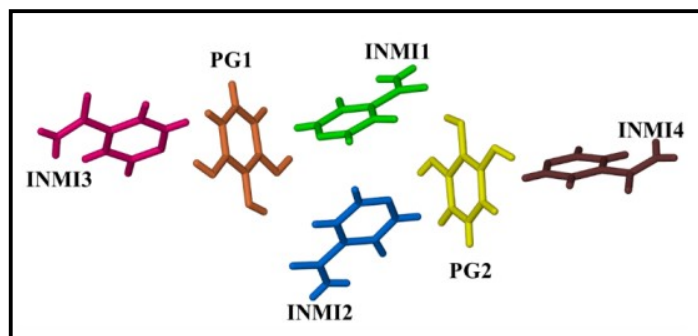
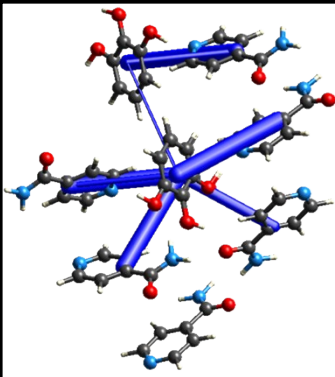
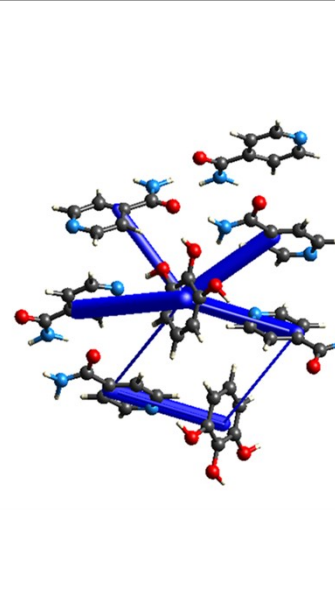


Figure S10 All unique molecules of **PGINMI12** shown by different colors in the unit cell, are considered for calculating interaction energies.



N	Symp	R	Electron Density	E_ele	E_pol	E_dis	E_rep	E_tot
2	-x, y+1/2, -z	7.33	B3LYP/6-31G(d,p)	-2.3	-0.4	-9.2	8.8	-5.3
1	-	7.83	B3LYP/6-31G(d,p)	-1.4	-0.3	-2.1	0.1	-3.4
2	x, y, z	5.80	B3LYP/6-31G(d,p)	-1.3	-1.0	-9.4	1.9	-9.1
1	-	7.14	B3LYP/6-31G(d,p)	-64.7	-15.6	-11.9	74.8	-44.1
1	-	5.18	B3LYP/6-31G(d,p)	-29.5	-6.8	-17.3	37.7	-28.0
1	-	5.50	B3LYP/6-31G(d,p)	-39.4	-9.6	-17.2	37.8	-40.4
1	-	5.41	B3LYP/6-31G(d,p)	-8.2	-1.2	-19.5	20.4	-14.0
1	-	6.07	B3LYP/6-31G(d,p)	-3.2	-1.4	-13.0	17.0	-5.2
1	-	7.24	B3LYP/6-31G(d,p)	-65.5	-15.2	-11.8	81.4	-40.4

Figure S11 Total interaction energy calculation of **PG1** in **PGINMI12**.



N	Symp	R	Electron Density	E_ele	E_pol	E_dis	E_rep	E_tot
0	-x, y+1/2, -z	7.33	B3LYP/6-31G(d,p)	-2.3	-0.4	-9.2	8.8	-5.3
0	-	7.83	B3LYP/6-31G(d,p)	-1.4	-0.3	-2.1	0.1	-3.4
0	x, y, z	5.80	B3LYP/6-31G(d,p)	-1.3	-1.0	-9.4	1.9	-9.1
0	-	7.14	B3LYP/6-31G(d,p)	-64.7	-15.6	-11.9	74.8	-44.1
0	-	5.18	B3LYP/6-31G(d,p)	-29.5	-6.8	-17.3	37.7	-28.0
0	-	5.50	B3LYP/6-31G(d,p)	-39.4	-9.6	-17.2	37.8	-40.4
0	-	5.41	B3LYP/6-31G(d,p)	-8.2	-1.2	-19.5	20.4	-14.0
0	-	6.07	B3LYP/6-31G(d,p)	-3.2	-1.4	-13.0	17.0	-5.2
0	-	7.24	B3LYP/6-31G(d,p)	-65.5	-15.2	-11.8	81.4	-40.4
2	x, y, z	5.80	B3LYP/6-31G(d,p)	-0.7	-1.3	-10.0	2.6	-8.8
2	-x, y+1/2, -z	7.47	B3LYP/6-31G(d,p)	-0.9	-0.4	-6.1	4.7	-3.6
1	-	5.73	B3LYP/6-31G(d,p)	-7.0	-1.0	-15.3	17.5	-10.6
1	-	5.17	B3LYP/6-31G(d,p)	-32.0	-7.1	-17.7	44.0	-27.3
1	-	7.02	B3LYP/6-31G(d,p)	-2.0	-0.7	-5.5	1.8	-6.3
1	-	6.99	B3LYP/6-31G(d,p)	-68.3	-16.9	-13.4	83.5	-44.7
1	-	7.34	B3LYP/6-31G(d,p)	-61.9	-14.2	-10.0	74.7	-38.5
1	-	5.45	B3LYP/6-31G(d,p)	-41.0	-9.8	-17.9	38.2	-42.6
1	-	6.06	B3LYP/6-31G(d,p)	-0.8	-0.3	-10.8	8.0	-5.5
1	-	5.61	B3LYP/6-31G(d,p)	-5.0	-1.7	-19.0	22.2	-9.4

Figure S12 Total interaction energy calculation of **PG2** in **PGINMI12**.

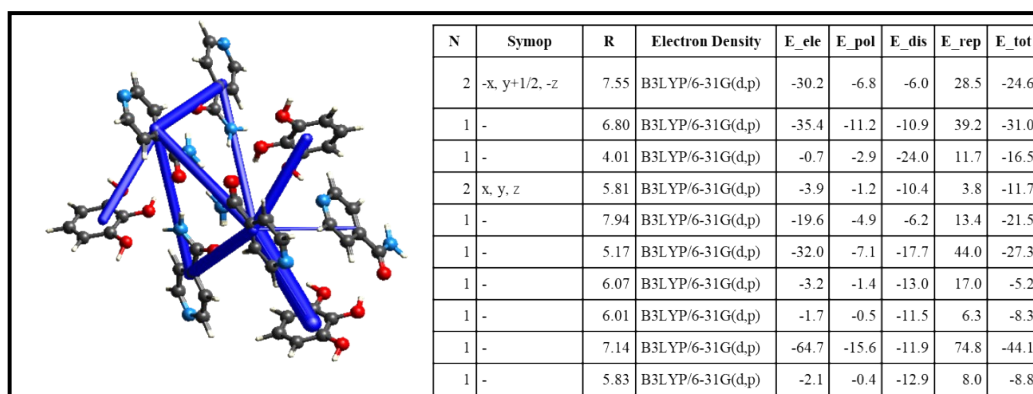


Figure S13 Total interaction energy calculation of INMI1 in PGINMI12.

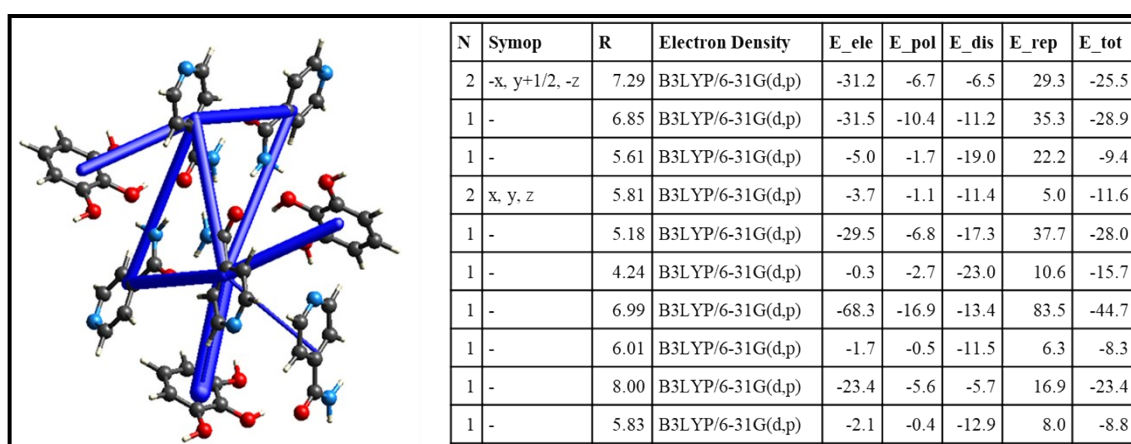


Figure S14 Total interaction energy calculation of INMI2 in PGINMI12.

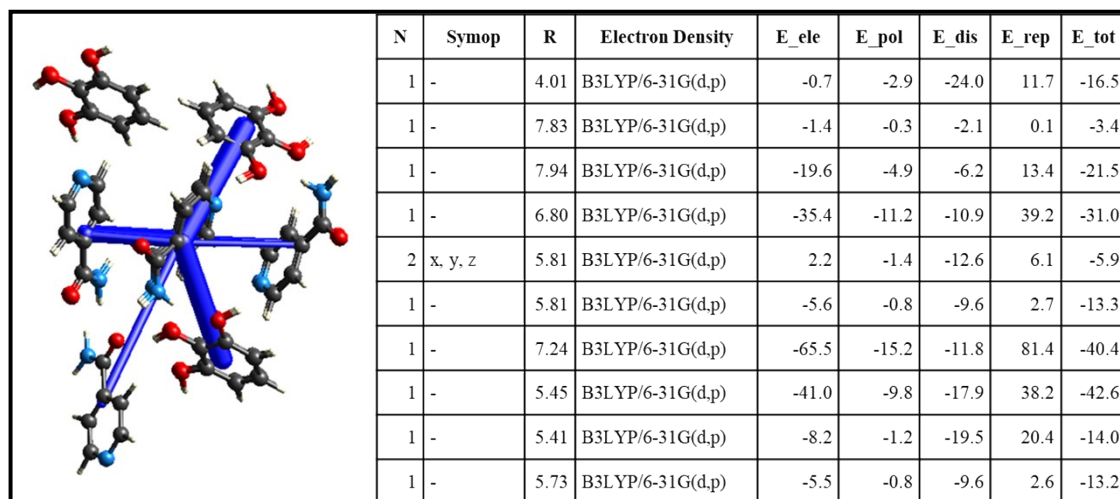
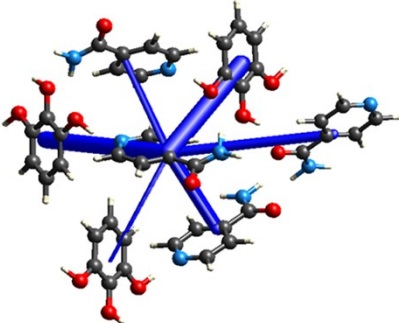


Figure S15 Total interaction energy calculation of INMI3 in PGINMI12.



N	Symp	R	Electron Density	E_ele	E_pol	E_dis	E_rep	E_tot
1	-	4.24	B3LYP/6-31G(d,p)	-0.3	-2.7	-23.0	10.6	-15.7
1	-	5.50	B3LYP/6-31G(d,p)	-39.4	-9.6	-17.2	37.8	-40.4
2	x, y, z	5.80	B3LYP/6-31G(d,p)	1.1	-1.3	-12.3	6.9	-6.3
1	-	7.34	B3LYP/6-31G(d,p)	-61.9	-14.2	-10.0	74.7	-38.5
1	-	5.73	B3LYP/6-31G(d,p)	-5.5	-0.8	-9.6	2.6	-13.2
1	-	6.06	B3LYP/6-31G(d,p)	-0.8	-0.3	-10.8	8.0	-5.5
1	-	5.73	B3LYP/6-31G(d,p)	-7.0	-1.0	-15.3	17.5	-10.6
1	-	8.00	B3LYP/6-31G(d,p)	-23.4	-5.6	-5.7	16.9	-23.4
1	-	6.85	B3LYP/6-31G(d,p)	-31.5	-10.4	-11.2	35.3	-28.9
1	-	7.02	B3LYP/6-31G(d,p)	-2.0	-0.7	-5.5	1.8	-6.3
1	-	5.81	B3LYP/6-31G(d,p)	-5.6	-0.8	-9.6	2.7	-13.3

Figure S16 Total interaction energy calculation of **INMI4** in **PGINMI12**.

PGINMI21 exhibits brittle behaviour in response to applied force. It has three independent molecules in the unit cell which are considered for the calculation of total interaction energies.

All these molecules are grown within the 3.8Å radius

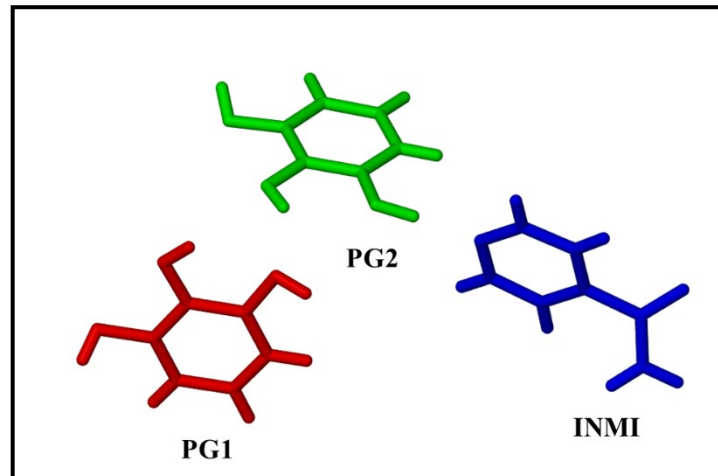


Figure S17 All unique molecules of **PGINMI21** shown by different colors in the unit cell, consider for calculating interaction energies.

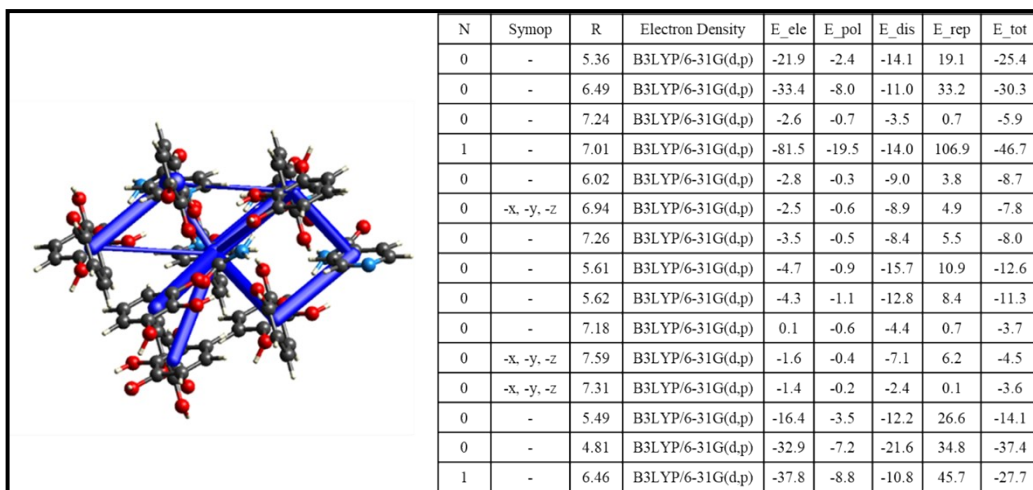


Figure S18 Total interaction energy calculation of PG1 in PGINMI21.

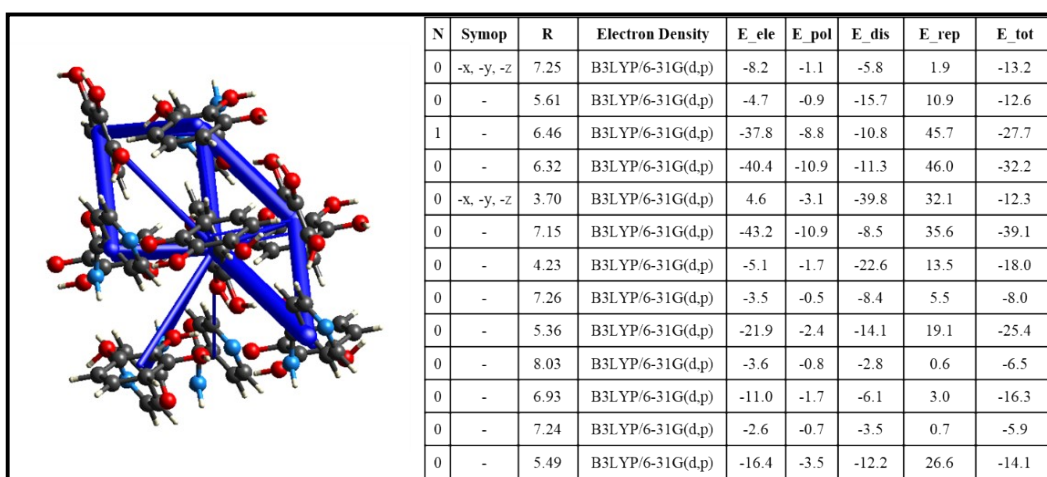


Figure S19 Total interaction energy calculation of PG2 in PGINMI21.

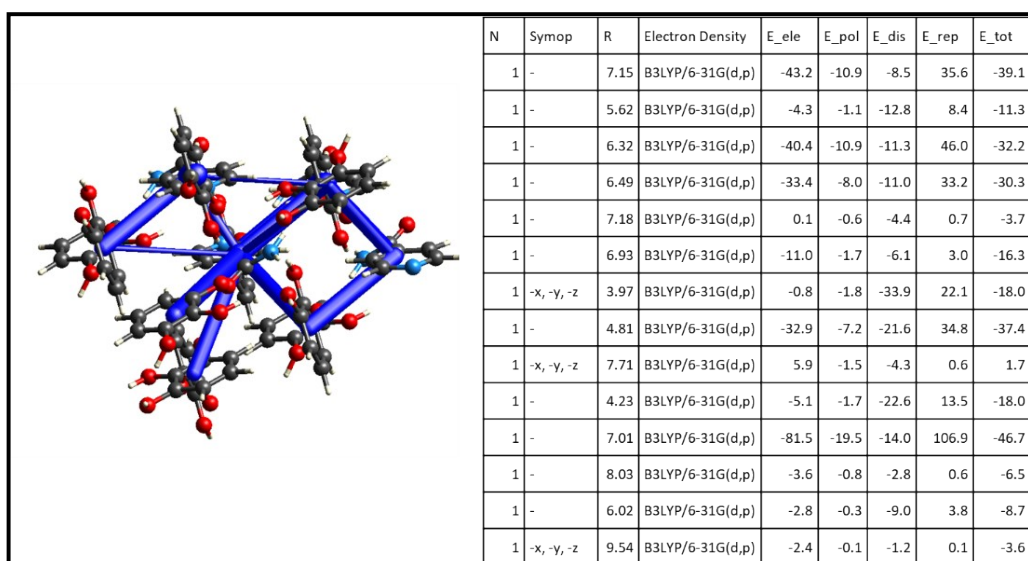
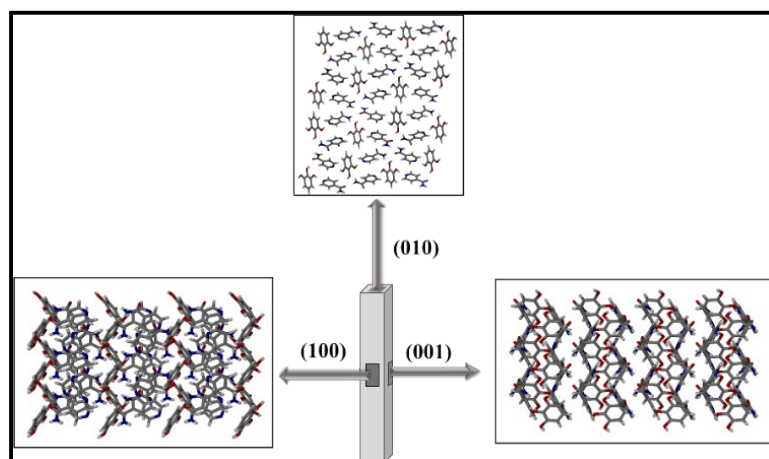
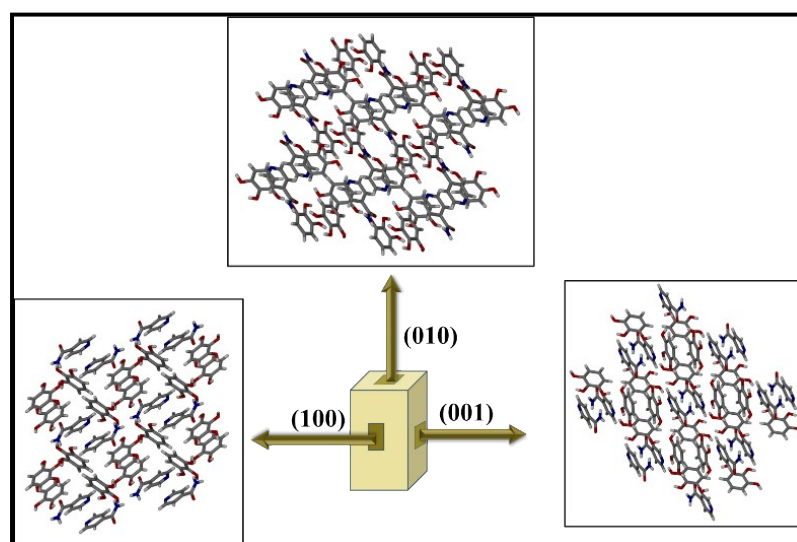


Figure S20 Total interaction energy calculation of INMI in PGINMI21.

8) Crystal Morphology with Face indices



(a)



(b)

Figure S21: Crystal morphology with face indices and packing of the molecules on (010), (001) and (100) faces, (a) **PGINMI12** and (b) **PGINMI21**.

NOTE: Structure graphics shown in the figures were created using the X-Seed software package version 4.0⁶

9) Thermal ellipsoid plot of the asymmetric unit

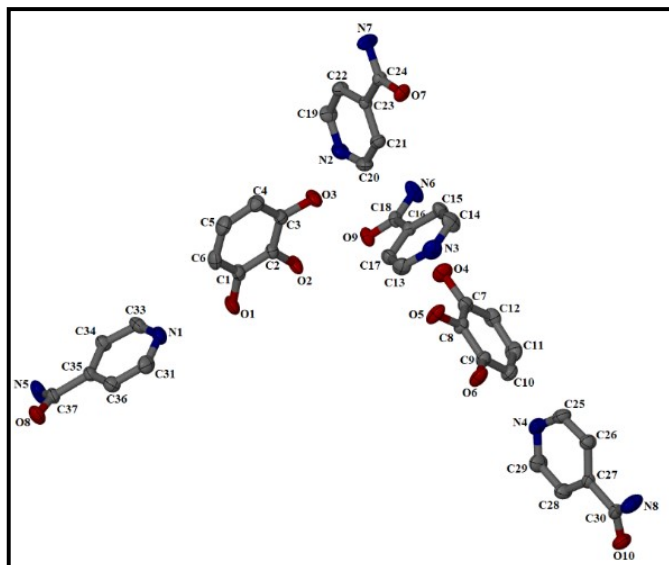


Figure S22 Thermal ellipsoid plots of asymmetric of **PGINMI12**, atoms are calculated with 40% probability and H-atoms are removed for the clarity of picture.

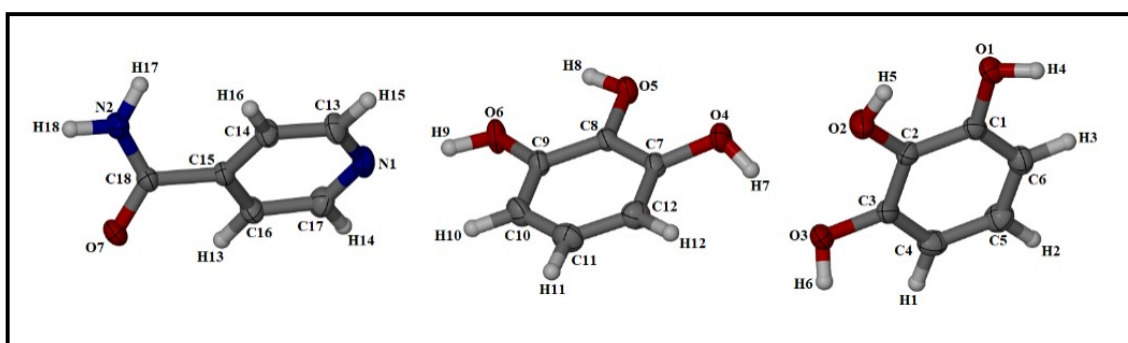
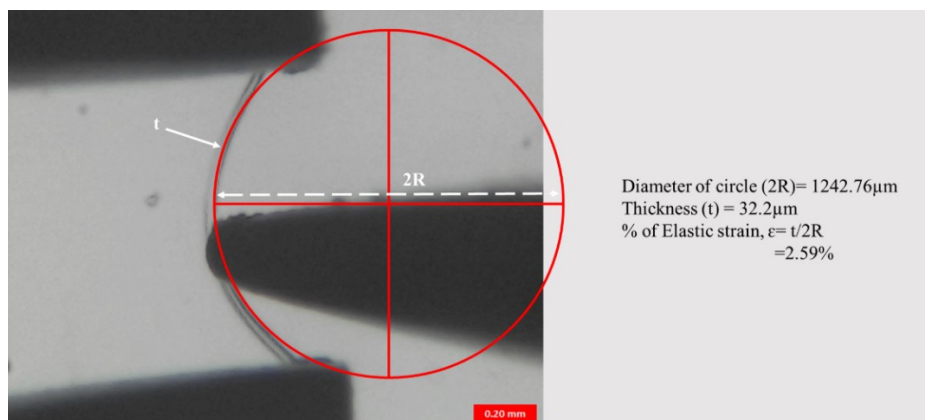


Figure S23 Thermal ellipsoid plots of asymmetric of **PGINMI21**. The atoms are calculated with 50% probability.

10) Calculation of Elastic Strain



1. R. Thakuria, S. Cherukuvada and A. Nangia, *Cryst. Growth Des.*, 2012, **12**, 3944
2. SAINT; Bruker AXS Inc., Madison, Wisconsin, USA, **2013**. SADABS; Bruker AXS Inc., Madison, Wisconsin, USA, **2012**.
3. Sheldrick, G. M. SHELXTL v **2014/5**; <http://shelx.uni-ac.gwdg.de/SHELX/index.php>.
4. A. L. Spek, *Acta Crystallogr., Sect. D*, **2009**, 65, 148.
5. D. Jayatilaka, and M. A. Spackman, *J. Appl. Cryst.*, 2021, **54**, 1006.
6. L. J. Barbour, X-Seed. *J. Supramol. Chem.*, 2001, **1**, 189.